Eur. Phys. J. D (2014) 68: 59
DOI: 10.1140/epjd/e2014-40749-7

THE EUROPEAN PHYSICAL JOURNAL D

Regular Article

Time-efficient numerical simulation of diatomic molecular spectra

Robert Beuc, Mladen Movre, and Berislav Horvatić[a]

Institute of Physics, Bijenička cesta 46, 10000 Zagreb, Croatia

Received 28 November 2013 / Received in final form 21 January 2014
Published online 27 March 2014 –

Abstract. We present a quantum-mechanical procedure for calculating the photoabsorption spectra of diatomic molecules, entirely based on the Fourier grid Hamiltonian method for obtaining energies and the corresponding wave functions. Discrete and continuous spectrum contributions, which are the result of transitions between bound, free, and quasibound states of diatomic molecules were treated on the same footing. Using the classical Franck-Condon principle and the stationary-phase approximation, we also developed a "semiquantum" simulation method of the spectrum which allows an extremely time-efficient numerical algorithm, reducing the computer time by up to four orders of magnitude. The proposed method was tested on the absorption spectra of potassium molecules.

1 Introduction

Photoabsorption spectra of diatomic molecules are well understood. Given the relevant potential curves and the associated transition dipole moment functions, one has to solve the radial Schrödinger equation, evaluate the required matrix elements and calculate state-to-state cross sections [1]. Fully quantum-mechanical calculations have been carried out for a number of molecules (see for example [1–6]).

For heavier alkali-metal dimers at elevated temperatures (several hundreds up to few thousands K), the absorption spectrum of the e.g. A-X transition is extremely dense due to the numerous rovibrational levels populated in the ground state. Even the most powerful Doppler limited techniques are not able to fully resolve the rotational structure. Recently, the low-resolution absorption spectroscopy was demonstrated as a valuable tool for checking the accuracy of molecular electronic structure calculations [7].

There are four possible contributions to the absorption spectrum corresponding to various types of transitions among the lower and upper bound and/or continuum states, viz. bound-bound (b-b), bound-free (b-f), free-bound (f-b), and free-free (f-f). The simplest treatment of continuum states consists in discretizing the continuum. It is discretized over a finite basis, and approximate continuum wave functions are determined only at some positive energies. The main advantage of the approach is its simplicity. In the present work energies and wave functions for rovibrational eigenstates were determined within the framework of the Fourier grid Hamiltonian (FGH) method [8,9].

The theoretical framework being well-defined, the main effort left is either numerical implementation or additional approximations, or both.

In this report we address both of these persisting challenges, hopefully in a nontrivial, novel, and, above all, a useful and usable way.

In Section 2.1 we present a quantum-mechanical procedure for calculating the photoabsorption spectra of diatomic molecules entirely based on the Fourier grid Hamiltonian method for obtaining energies and the corresponding wave functions. The method enables the analysis of spectra in ultracold conditions, spectra of molecules adsorbed on cold helium droplets, as well as the analysis of spectra of hot gases, either in laboratory conditions or in the atmospheres of cold stars. The studies mentioned above could be used in applied research as well (e.g., design and optimization of efficient light sources).

In Section 2.2 we present a numerically efficient method for the calculation of optical spectra of diatomic molecules which unites good properties of the semiclassical and quantum-mechanical approach. Using the classical Franck-Condon principle and the stationary-phase approximation, we developed a "semiquantum" simulation method of the spectrum, which allows a time-efficient algorithm, suitable for use in the spectroscopic data analysis. The approximation is found in very good agreement with fully quantum-mechanical calculations, while its consumption of computer time is lower by four orders of magnitude.

In Section 3 we give the technical details of the numerical calculations and present the results. Theoretical

[a] e-mail: horvatic@ifs.hr

results we obtained were tested by comparison with experimental absorption spectra of potassium molecules at different temperatures. The agreement is found to be quite respectable for both methods.

Section 4 comprises a brief summary of the results and a few comments on further prospects and improvements.

The main steps of the somewhat lengthy derivation of the "semiquantum" formula via WKB wavefunctions are outlined in the Appendix.

2 The thermally averaged absorption coefficient

The photoabsorption process is usually quantified in terms of the thermally averaged absorption coefficient $k(\nu,T)$. Here, ν is the frequency of the absorbed photon and T is the temperature.

Let Λ'' and Λ' label the lower and the upper state, respectively, Λ being the axial component of the electronic angular momentum. Let $V_\Lambda(R)$ be the *interaction* potential for the relevant electronic state, with the potential energy measured with respect to the dissociation limit E_Λ^∞ of the corresponding potential-energy curve, i.e., $V_\Lambda(R) \to 0$ as $R \to \infty$. Let $\varepsilon_{v,J,\Lambda} = E_\Lambda^\infty + E_{v,J,\Lambda}$ denote the energy of a bound state ($E_{v,J,\Lambda} < 0$, v discrete: $v = 0, 1, 2, \ldots, v_{\max}(J)$) or a continuum one ($E_{v,J,\Lambda} > 0$, v continuous: $v \in [v_{\rm diss}(J), \infty)$), v being the vibrational quantum number and J the rotational quantum number. Here $v_{\max}(J)$ denotes the highest truly bound level, i.e. the quasibound states (resonances) are considered as a part of the continuum. The meaning of the continuous quantum number v is the following: there are dv states between v and $v + dv$. Alternatively, continuum states may be labeled with their asymptotic kinetic energy ε (note that the asymptotic energy ε is decoupled from J, whereas $E_{v,J,\Lambda}$ depends on both v and J). The number of states having energy ε between ε and $\varepsilon + d\varepsilon$ is $dv = \rho(\varepsilon)d\varepsilon$, where $\rho(\varepsilon)$ is the density of states.

The transition energy $\varepsilon_{v',J',\Lambda'} - \varepsilon_{v'',J'',\Lambda''}$ is:

$$h\nu_{tr} = h\nu_0 + \left(E_{v',\,J',\,\Lambda'} - E_{v'',\,J'',\,\Lambda''}\right), \qquad (1)$$

where $h\nu_0 = E_{\Lambda'}^\infty - E_{\Lambda''}^\infty$.

2.1 Quantum calculation on the Fourier grid

Solving the relevant radial Schrödinger equation on the grid one obtains a set of discrete energies effectively describing a *confined* molecule, "a molecule in a box", and the entire spectrum is of the b-b type. The b-b contribution to the thermally averaged absorption coefficient [2,5] may be put in the form more convenient for further discussion,

$$k(\nu,\,T) = C(\,\nu,T)I(\nu,T), \qquad (2)$$

where the first term

$$C(\,\nu,T) = N_a N_b w \frac{8\pi^3\nu}{3hc}\left(\frac{h^2}{2\pi\mu k_B T}\right)^{3/2} \times \frac{(2-\delta_{0,\,\Lambda'+\Lambda''})}{(2-\delta_{0,\,\Lambda''})}\,\frac{2S+1}{(2S_a+1)\,(2S_b+1)} \qquad (3)$$

contains all the statistical factors pertaining to atomic and molecular electron states, including various partition functions, as expounded in detail in references [1,5], and obeys a simple linear dependence on frequency ν. Here $w = 1$ or $1/2$ for heteronuclear or homonuclear dimers, respectively, N_a and N_b denote the atomic number densities, S_a (S_b) and S the atomic and molecular spin quantum numbers, respectively. The function $I(\nu,T)$ comprises the essential information specific to a particular molecule under consideration,

$$I(\nu,\,T) = \sum_J (2J+1) \sum_{v'',v'} \exp\left(-\frac{E_{v'',J,\,\Lambda''}}{k_B T}\right) \times \left|\langle \Phi_{v'',J,\Lambda''}\,|D(R)|\,\Phi_{v',J,\Lambda'}\rangle\right|^2 g\left(\nu-\nu_{tr}\right), \qquad (4)$$

where $\Phi_{v,J,\Lambda}$ is the radial wave function, $D(R)$ the electronic transition dipole moment, and $g(\nu)$ a line shape function. In what follows we neglect the natural and Doppler broadening and approximate the line shape function with the Dirac delta function. Writing equation (4) we also assumed the applicability of the Q-branch approximation [4], $J' = J'' \equiv J$ (of course, this approximation should not be used for ultralow temperatures).

Equation (4) gives a fine-grained description ("rotational comb") of the spectrum of a confined molecule. In order to simulate experimental spectra, equation (4) should be convoluted with a function $g_{\rm instr}(\nu)$, normalized to unity, representing the instrumental profile. The experimental resolution is characterized by the width of the instrumental profile (usually FWHM, where greater FWHM means lower resolution). The convoluted spectrum is smeared out over the width of the instrumental profile, and if the typical spacing of the rotational lines (within a vibrational band) is smaller than the experimental resolution width, the observed spectrum appears continuous.

Our numerical technique provides the absorption coefficient at discrete energies only. A continuous part of the absorption coefficient may be recovered by folding equation (4) with a smearing function $g_{\rm smear}(\nu)$ which usually involves a width parameter σ. This parameter should simulate the finite energy resolution of the detectors and therefore should be fixed by the experimental conditions. In practice, however, σ is often regarded as a free parameter, while it also corrects for the discretization imposed by the confinement.

Equation (4), together with a judiciously chosen smearing function $g\left(\nu-\nu_{tr}\right)$, represents a full quantum-mechanical recipe for calculating the absorption spectra of diatomic molecules, entirely based on the FGH method. For every J the energies and the corresponding wave functions are obtained in a single diagonalization of

the Hamiltonian matrix $H = T + V$, whose kinetic and potential parts are given by the matrices [8]

$$T_{i,j} = \frac{\hbar^2}{2\mu\Delta R^2} \begin{cases} \frac{\pi^2}{3} - \frac{1}{2i^2} & i = j \\ (-1)^{i-j} \frac{8ij}{(i^2-j^2)^2} & i \neq j \end{cases}, \tag{5a}$$

$$V_{i,j} = \left[V_\Lambda(R_i) + \frac{\hbar^2}{2\mu} \frac{J(J+1) - \Lambda^2}{R_i^2} \right] \delta_{i,j}, \tag{5b}$$

where μ is the reduced mass, R_i the grid points, and ΔR the step size. The wave functions are determined on a uniform grid with N_p points and normalized as:

$$\sum_{i=1}^{N_p} \Phi^*_{v,J,\Lambda}(R_i)\ \Phi_{v,J,\Lambda}(R_i) = 1 \tag{6}$$

and the matrix elements of the transition dipole moment $D(R)$ are computed as:

$$\langle \Phi_{v'',J'',\Lambda''} | D(R) | \Phi_{v',J',\Lambda'} \rangle = \sum_{i=1}^{N_p} \Phi^*_{v'',J'',\Lambda''}(R_i) D(R_i) \Phi_{v',J',\Lambda'}(R_i). \tag{7}$$

Once obtained, the energies and dipole moments are used in equation (4) for the calculation of the thermally averaged absorption coefficient for any temperature of interest.

Discrete and continuous spectrum contributions, which are the result of transitions between bound, free, and quasibound states of diatomic molecules, were treated on the same footing. The energy levels of the quasibound states (resonances) are stable against the change of the size of the grid (the size of the confining box) whereas the energies of the background (quasi)continuum states decrease with growing grid size. If necessary, the quasibound states may be easily identified either by the inspection of the wave functions (well localized within the potential well) or some matrix elements ($\langle \Phi_{v,J,\Lambda} | R^{-2} | \Phi_{v,J,\Lambda} \rangle$ for example). We stress once more that all transitions between bound, free, and quasibound states of diatomic molecules are accounted for by using the FGH method together with expression (4). Therefore, within *this* scheme, one does not have to identify the quasibound states at all, nor deal with them in any special way.

Usually, hundreds of J values are required and the number of points N_p is of the order of 10^3. Except in the case of an extremely high resolution, most of the detailed information is actually smeared out in the final spectrum. This is a circumstance that clearly allows some additional approximations, which in their turn can greatly reduce the computational time. One of the options is the one we propose next.

2.2 "Semiquantum" approximation

Treating all variables as continuous, the function $I(\nu, T)$ given by equation (4) may be written as:

$$\begin{aligned} I(\nu,T) \approx h \int_0^\infty dY \int_{\varepsilon''_{\min}}^\infty d\varepsilon'' \exp\left(-\frac{\varepsilon''}{k_B T}\right) \\ \times \int_{\varepsilon'_{\min}}^\infty d\varepsilon' \left| \langle \Psi_{\varepsilon'',Y,\Lambda''} | D(R) | \Psi_{\varepsilon',Y,\Lambda'} \rangle \right|^2 \\ \times \delta(\varepsilon'' + h\nu - h\nu_0 - \varepsilon') \\ = h \int_{\varepsilon''_{\min}}^\infty d\varepsilon'' \exp\left(-\frac{\varepsilon''}{k_B T}\right) \int_0^\infty dY \\ \times \left| \langle \Psi_{\varepsilon'',Y,\Lambda''} | D(R) | \Psi_{\varepsilon''+h\nu-h\nu_0,Y,\Lambda'} \rangle \right|^2 \\ \times \Theta(\varepsilon'' + h\nu - h\nu_0 - \varepsilon'_{\min}). \end{aligned} \tag{8}$$

Here we introduced a new variable $Y = J(J+1)$ and made use of the fact that any unity-normalized bound-state wave function Φ_v can be turned into an energy-normalized wave function $\Psi_\varepsilon = |\partial E_{v,J,\Lambda}/\partial v|^{-1/2}_{E_{v,J,\Lambda}=\varepsilon} \Phi_v$. The lower limit $\varepsilon_{\min}$ for the true continuum equals zero, but here we take the value of the minimum of the corresponding potential, treating the whole energy spectrum as continuous.

Now we proceed within the semiclassical approximation. The transitions are assumed to be "local" and "vertical", occuring only at the Condon points $R = R(\nu; \Lambda', \Lambda'') \equiv R_\nu$, satisfying the equation $V_{\Lambda'}(R) - V_{\Lambda''}(R) = h\nu$, and to contribute to the spectrum if and only if R_ν happens to be in the classically allowed region (CAR) of the phase space, defined by:

$$0 \leqslant Y \leqslant Y_M(\varepsilon''; R_\nu) \equiv \frac{2\mu R_\nu^2}{\hbar^2} \left[\varepsilon'' - V_{\Lambda''}(R_\nu) \right]. \tag{9}$$

Note that this condition restricts both Y and ε, thus resetting the above defined $\varepsilon_{\min}$'s to the corresponding CAR values $\varepsilon_{\min} = V_\Lambda(R_\nu)$. That is, we assume the validity of the classical Franck-Condon principle – that the dominant contributions to the matrix elements come from the narrow regions around the classically allowed Condon points. Thus, for ν satisfying $\varepsilon'' + h\nu - h\nu_0 - \varepsilon'_{\min} \geqslant 0$ one has:

$$\begin{aligned} I(\nu,T) \approx h \int_{\varepsilon''_{\min}}^\infty d\varepsilon'' \exp\left(-\frac{\varepsilon''}{k_B T}\right) \int_0^{Y_M(\varepsilon'';R_\nu)} dY \\ \times \left| \langle \Psi_{\varepsilon'',Y,\Lambda''} | D(R) | \Psi_{\varepsilon''+h\nu-h\nu_0,Y,\Lambda'} \rangle \right|^2, \end{aligned} \tag{10}$$

while otherwise $I(\nu, T) \equiv 0$ (for the sake of simplicity, we here assumed just a single Condon point R_ν).

Now, if one restricts the integrations over Y and ε'' to the CAR only, it is a matter of consistency to forsake the fully quantum-mechanical integrand as well and replace it with its semiclassical counterpart, i.e., calculate

$I(\nu,T)$ using the WKB wave functions, the stationary-phase approximation, and neglecting rapidly oscillating phase contributions. The main steps of the somewhat lengthy but rather straightforward derivation are outlined in the Appendix, with the result

$$I(\nu,T) \approx h\frac{2\mu k_B T}{\hbar^2}\int\limits_{\varepsilon''_{\min}}^{\infty} d\varepsilon'' \exp\left(-\frac{\varepsilon''}{k_B T}\right) \times \left|\left\langle \Psi_{\varepsilon'',0,\Lambda''} \left| RD(R) \right| \Psi_{\varepsilon''+h\nu-h\nu_0,0,\Lambda'}\right\rangle\right|^2. \quad (11)$$

Turning back to unity-normalized wave functions $\Phi_{v,J,\Lambda}$, one finally obtains:

$$I(\nu,T) \approx \frac{2\mu k_B T}{\hbar^2}\int\limits_0^{\infty} dv'' \int\limits_0^{\infty} dv' \exp\left(-\frac{E_{v'',0,\Lambda''}}{k_B T}\right) \times \left|\left\langle \Phi_{v'',0,\Lambda''} \left| RD(R) \right| \Phi_{v',0,\Lambda'}\right\rangle\right|^2 \delta(\nu-\nu_{tr}). \quad (12)$$

Note that the integration over v' is of a formal nature due to the presence of the delta function. Given a partition $P = \{[0,v_1),[v_1,v_2),\ldots,[v_{n-1},v_n]\}$, where $0 < v_1 < \ldots < v_n$, one can approximate the integrals by the (left) Riemann sum and obtain a quantum-like ("quasiquantum" or "semiquantum") expression. Since solving the relevant Schrödinger equation on the grid yields a discrete representation of the continuum, the latter may be used as the very set $\{v_i\}$ defining the partition P. Furthermore $v_{i+1} = v_i + 1$. Finally one may write

$$I(\nu,T) \approx \frac{2\mu k_B T}{\hbar^2}\sum_{v'',v'} \exp\left(-\frac{E_{v'',0,\Lambda''}}{k_B T}\right) \times \left|\left\langle \Phi_{v'',0,\Lambda''} \left| RD(R) \right| \Phi_{v',0,\Lambda'}\right\rangle\right|^2 g(\nu-\nu_{tr}). \quad (13)$$

A smearing function $g(\nu)$ again simulates the finite energy resolution of the detectors and also corrects for the (artificial) discretization imposed by the confinement.

Deriving equation (13) we first assumed a single Condon point (which is true for e.g. the potassium B-X band). We show in the Appendix that equations (10) and (13) share the same semiclassical limit for *any* number of Condon points. A few words are in order on the appearance of $\langle \Phi_{v'',0,\Lambda''}|RD(R)|\Phi_{v',0,\Lambda'}\rangle$ in equation (13). Whenever one deals with a localized transition, the stationary-phase argument allows the approximation

$$\langle \Phi_{v'',0,\Lambda''}|RD(R)|\Phi_{v',0,\Lambda'}\rangle \approx R_\nu \langle \Phi_{v'',0,\Lambda''}|D(R)|\Phi_{v',0,\Lambda'}\rangle.$$

Deriving equation (13) we reverse the argument and write

$$R_\nu \langle \Phi_{v'',0,\Lambda''}|D(R)|\Phi_{v',0,\Lambda'}\rangle \approx \langle \Phi_{v'',0,\Lambda''}|RD(R)|\Phi_{v',0,\Lambda'}\rangle.$$

In order to evaluate equation (13), one needs to know the vibrational energies and the corresponding wave functions for $J = 0$ only. The set of transition frequencies ν_{tr} is finite and discrete. Prior to smearing, the spectrum is given only at these discrete frequencies.

We dubbed the equation (13) "semiquantum" because it comprises transition dipole moment matrix elements that are fully quantum expressions (i.e., calculated with fully quantum eigenstates) and the summations over v'' and v' are *not* approximated by integrals (or in any other way), but the whole expression itself is just different from its truly quantum counterpart, equation (4).

There are indeed several plausible ways to introduce (or "derive") the semiquantum expression (13) and here we presented just the most straightforward one. We showed that the fully quantum expression (4) and the semiquantum expression (13) have the same semiclassical limit (for an arbitrary number of Condon points). This is only the first step. Testing it on real spectra shows that equation (13) fares rather well even far away from that limit, deep into the fully quantum region.

Although both the standard semiclassical approximation (SCA, see Ref. [10]) and our semiquantum approximation (SQA) are based on the same classical intuition, there are some important differences. SCA does not give the rovibrational molecular structure of the spectrum bands, but agrees perfectly with the averaged-out quantum-mechanical spectra. On the other hand, SQA does reproduce the vibrational structure of rotationless potentials and does not require the explicit determination of Condon points (which in the case of two or more Condon points may make the procedure more complicated). Neither is the proximity of a Condon point to a classical turning point an issue. The matrix element takes care of all that "automatically".

A remark is due here on the issue of the Q-branch approximation ($J' = J'' \equiv J$) with regard to ultralow temperatures. Our fully quantum-mechanical calculations do not rely on it in any essential way – one can give up this approximation at the only cost of just tripling the computer time. For ultracold temperatures that is, of course, no problem at all. For medium-to-high temperatures, however, it does become rather inconvenient, so we stick to the Q-branch approximation, which is fully justified for this temperature range.

Regarding the SQA, the Q-branch approximation is essential for its "derivation". But, on the other hand, for ultralow temperatures we do not need the SQA in the first place, since the full quantum-mechanical calculation is fast enough.

We first tested the SQA on the absorption spectra of potassium molecules, and for several good reasons at that, viz. for K_2 one has high-quality potentials and transition dipole moments, as well as both good experimental data and previous quantum [5] and semiclassical [11] calculations to compare with. Also, in K_2 all four types of transitions (b-b, b-f, f-b, f-f) are sufficiently pronounced. All this makes K_2 a convenient choice for a case study of the proposed method.

3 Methods and results

In the major part of the theoretical simulations presented here we used ab initio potential energy functions and the

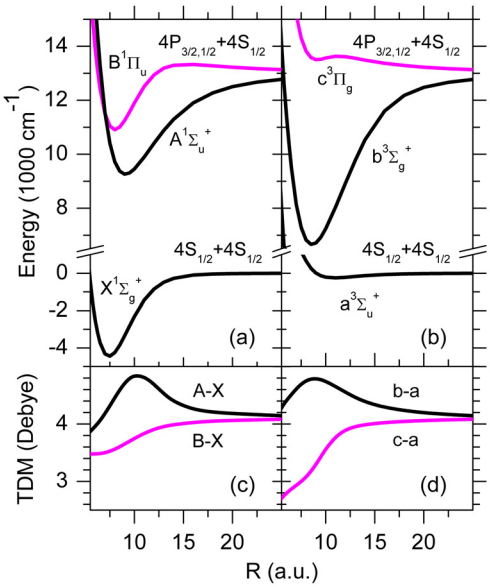

Fig. 1. Potential curves of the K_2 molecule for the ground state and the first excited states, and the associated transition dipole moments (TDM) used in reference [11].

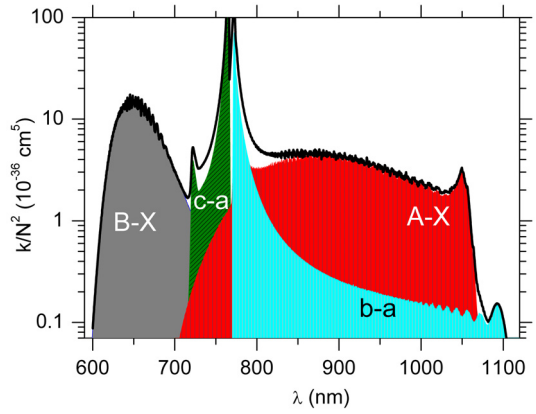

Fig. 2. Contributions to the fully quantum-mechanical simulation of the total K_2 spectrum for the temperature $T = 985$ K.

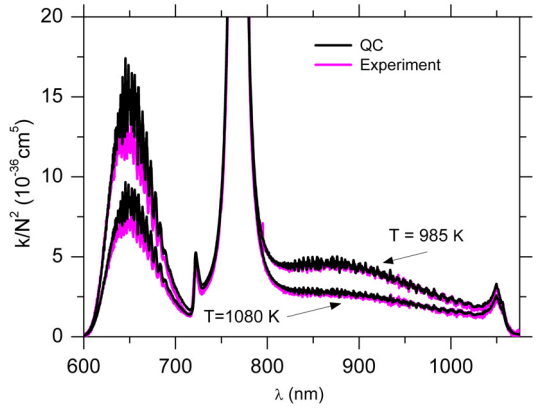

Fig. 3. Simulated spectra (fully quantum-mechanical calculations – QC) for optimal fitting temperatures 985 K and 1080 K compared to the experimental spectra from reference [10]. The corresponding experimentally determined temperatures are 960 ± 30 K and 1025 ± 30 K, respectively.

relevant transition dipole moments [12]. We also used the available experimentally determined potential functions for the singlet transitions [13–16]. For further details see reference [11]. Throughout the paper the states of a given symmetry conforming to the standard $^{2S+1}\Lambda_{g/u}^{+/-}$ Hund's case-(a) notation are labeled in order of increasing energy as X, A, B, and a, b, c, for singlet and triplet states, respectively.

Considering the manifolds of the interaction potential curves stemming from the 4 ^{2}S + 4 ^{2}S and 4 ^{2}S + 4 ^{2}P asymptotes (see Fig. 1) we have taken into account all transitions which give contributions to the absorption in the wavelength region of interest. In Figure 1a we show the singlet states X, A, B, and in Figure 1c the corresponding A-X and B-X transition dipole moments (TDM). The potential of the excited B state has a potential barrier at $R = 15.25a_0$, of the height of 308 cm^{-1} (with respect to the dissociation limit $E^{\infty}_{\Lambda=1}$), so even for $J = 0$ this potential supports a number of quasibound states. Figure 1b shows the triplet a, b, and c states, and Figure 1d the b-a and c-a transition dipole moments.

We used the variant of the Fourier grid method first proposed by Colbert and Miller [8] and later used and discussed by Willner et al. [9]. The grid of a finite size is tantamount to confining the radial motion to the range spanned by the grid. The method yields a discrete set of continuum energies (a quasicontinuum) only, but in the range spanned by the grid the corresponding wave functions do represent the states of a true continuum, being just differently normalized. Only continuum states having a node at the outer boundary are retained.

The parameters of the grid (the step size ΔR and the number of points N_p) are estimated in the following way. Aiming to simulate the spectra for temperatures up to $T_{\max} = 3000$ K, we chose the local radial kinetic energy cutoff amounting to $\varepsilon_{kin}/hc = 8000$ cm^{-1}. The step size is then given by $\Delta R = h/\left(n_B\sqrt{2\mu\varepsilon_{kin}}\right)$, where n_B is the number of grid points per de Broglie wavelength. We obtained stable numerical results already for $n_B = 3$. In order to get closer to the atomic line centre, we put the last grid point at $40a_0$. Finally, we used $N_p = 970$ points, ranging from $0.04a_0$ to $40a_0$. We summed over J up to $J_{\max} = 1000$, where, $J_{\max}$ was estimated according to $\hbar^2 J^2_{\max}/2\mu R^2_{N_p} \cong k_B T_{\max}$. The calculated spectrum is collected in bins of the size $\Delta\nu/c = 6$ cm^{-1}, and no further smoothing was attempted.

The fully quantum-mechanical spectrum, as well as the separate contributions of various molecular bands calculated for vapor temperature $T = 985$ K are presented in Figure 2. The reduced absorption coefficient k/N^2 is plotted versus the wavelength λ. The vibrational bands of the A-X and B-X bands are clearly seen. The rotational structure is very dense and appears continuous. In Figure 3 we compare experiment and theory for two experimental temperatures [11]. The overall agreement is

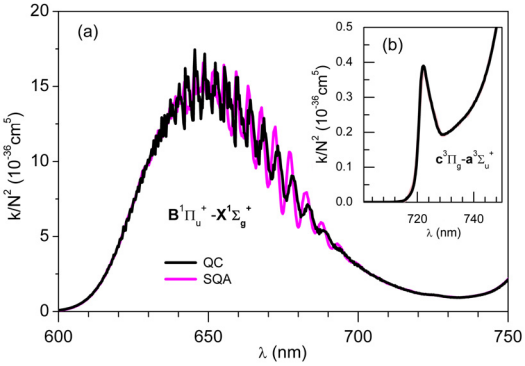

Fig. 4. Comparison of the semiquantum approximation (SQA) with the fully quantum calculations (QC) for (a) B-X band and (b) c-a band for the temperature $T = 985$ K.

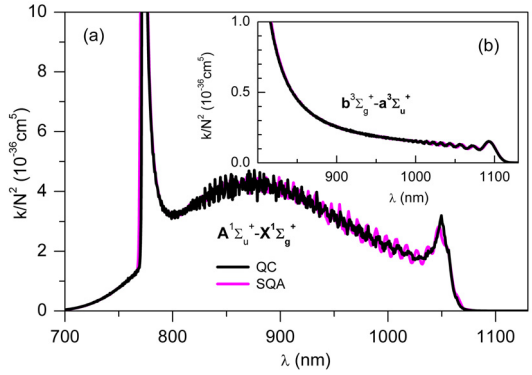

Fig. 5. Comparison of the semiquantum approximation (SQA) with the fully quantum calculations (QC) for (a) A-X band and (b) b-a band for the temperature $T = 985$ K.

satisfactory, all the structures are well reproduced. For example, although the simulated B-X band is somewhat higher in intensity, it closely resembles the experimentally observed spectrum. A slight increase in the simulated intensity may be attributed to the uncertainty of the ab initio transition dipole moments [7,11].

In summary, the fully quantum-mechanical procedure for calculating the absorption spectra of diatomic molecules, entirely based on the Fourier grid Hamiltonian method, presents a robust and reliable method which can be easily implemented in a high-level programming environment such as MATHEMATICA. One should stress that the FGH method yields the energies and wave functions of quasibound states as well.

A comment is due on the earlier quantum-mechanical calculations of the potassium spectrum by Talbi et al. [5]. Unfortunately we are unable to compare our results with theirs quantitatively, since we do not know what to make out of them. The spectra given in their Figures 3 and 4 are rather off our results quantitatively, which also means off the experimental ones, with which we are in quite respectable agreement. How much off also depends on the figure, since we estimate their Figures 3 and 4 to be mutually inconsistent by a factor of about two (according to the scales given there). Thus, e.g. their B-X band for 1000 K is on the average smaller by a factor of six or so than ours, if estimated from their Figure 3, while the comparison for 850 K gives a factor of three or so if estimated from their Figure 4. The scaling problem apart (which might have arisen from overlooking a factor of 2π or π, respectively), their B-X band is also *qualitatively* of a wrong shape, showing a shoulder on the blue side and a sharp peak, neither of which were observed either experimentally or in our simulations.

In the previous section we also proposed a semiquantum approximation to the absorption spectrum of a diatomic molecule. The semiquantum spectrum calculated according to equation (13) was collected in bins of the size $\Delta\nu/c = 10$ cm^{-1} and smoothed out. For a smoothing function we used a simple unity-normalized triangular profile having a width (FWHM) of 50 cm^{-1}.

Figure 4 shows the comparison of the semiquantum approximation (SQA) with the fully quantum calculations (QC) for the B-X and c-a bands, respectively. The SQA approximates QC favorably in the case of the c-a band and the agreement is satisfactory for the B-X band as well. The overall structure is well reproduced, especially the low-wavelength part dominated by the f–f transitions. The difference potential of the B-X transition has a single Condon point. The difference potential of the c-a transition has two or three real Condon points (depending on the transition energy), and since the excited c state is for the most part repulsive, the spectrum comprises mainly the f-f contributions.

In Figure 5 we compare SQA and QC for the A-X and b-a bands, respectively. One finds a very good agreement for the b-a band, and a satisfactory agreement for the A-X one. The difference potential of the A-X transition has two Condon points, and the spectrum of this transition for temperatures lower than a few thousand K comprises mainly the b-b contributions. The difference potential of the b-a transition has two Condon points, the depth of the ground a state is 248 cm^{-1}, while the excited b state has a deep minimum, so that the majority of transitions for temperatures higher than a few hundred K are of the f-b type.

Finally, in Figure 6 we compare SQA and QC for a range of temperatures, illustrating the influence of temperature change on the general shape of the photoabsorption profile. The overall agreement makes us confident that the proposed SQA offers a simple and time-efficient way to simulate the spectra of diatomic molecules, suitable for use in the spectroscopic data analysis.

4 Concluding remarks

We presented a fully quantum-mechanical procedure for calculating the photoabsorption spectra of diatomic molecules entirely based on the Fourier grid Hamiltonian method for obtaining energies and the corresponding wave functions. Theoretical results we obtained were

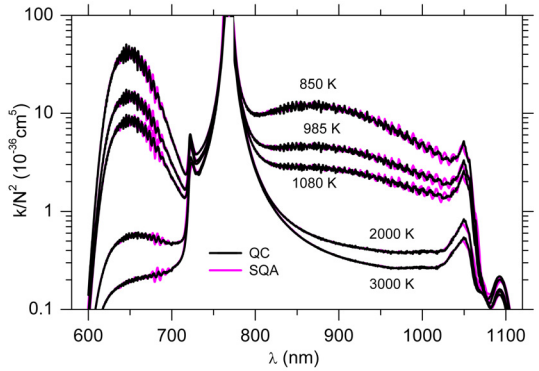

Fig. 6. Influence of temperature change on the overall shape of the photoabsorption profile. The temperatures range from 850 to 3000 K. The semiquantum approximation (SQA) is compared to the fully quantum calculations (QC).

tested by comparison with experimental absorption spectra of potassium molecules at different temperatures. The method enables the analysis of spectra in ultracold conditions, spectra of molecules adsorbed on cold helium droplets, as well as the analysis of spectra of hot gases, either in laboratory conditions or in the atmospheres of cold stars. The studies mentioned above could be used in applied research as well (e.g., design and optimization of efficient light sources).

In addition, we presented a numerically efficient method for the calculation of optical spectra of diatomic molecules which unites good properties of the semiclassical and quantum-mechanical approach. Using the classical Franck-Condon principle and the stationary-phase approximation, we developed a semiquantum simulation method of the spectrum, which allows a time-efficient algorithm, suitable for use in the spectroscopic data analysis. The standard semiclassical approximation does not give the rovibrational molecular structure of the spectrum bands, but agrees perfectly with the averaged-out quantum-mechanical spectra. The semiquantum approximation is in very good agreement with fully quantum calculations, while its consumption of computer time is lower by four orders of magnitude. For the calculation of the absorption spectrum of the B-X transition at the temperature of 985 K, the computer time required (quad-core 3 GHz processor, 8 GB RAM) amounts to 2675 s for the fully quantum calculations and only 0.16 s for the SQA. This means obtaining a fairly accurate spectrum at a glance.

For cesium molecules the SQA also yields more than reassuring results, which are deferred to a subsequent publication.

A disadvantage of this method is an unsatisfactory description of the discrete structure of molecular bands if a higher resolution of the spectra is required. However, even the low-resolution absorption spectroscopy may serve as a valuable tool for checking the accuracy of molecular electronic structure calculations [7]. Also, our preliminary investigation indicates that the semiquantum approximation might be further improved at a cost of merely doubling the computer time.

We acknowledge financial support from the Ministry of Science, Education, and Sports of the Republic of Croatia, Project No. 035-0352851-3213.

Appendix

Using energy-normalized wave functions in the standard WKB form,

$$\Psi_{\varepsilon,Y,\Lambda}(R) = \sqrt[4]{\frac{2\mu}{\pi^2\hbar^2}}\frac{1}{\sqrt[4]{\varepsilon - V_\Lambda(R,\,Y)}} \times \sin\left[\frac{\sqrt{2\mu}}{\hbar}\int_{R_t}^{R} dR'\sqrt{\varepsilon - V_\Lambda(R',\,Y)} + \frac{\pi}{4}\right], \tag{A.1}$$

where $V_\Lambda(R,\,Y) = V_\Lambda(R) + (\hbar^2 Y/2\mu R^2)$, and the standard approximation of neglecting the rapidly oscillating phase sums, one obtains the transition dipole matrix element in the form

$$\langle \Psi_{\varepsilon,Y,\Lambda''}\,|D(R)|\,\Psi_{\varepsilon+h\nu,Y,\Lambda'}\rangle \approx \frac{\sqrt{2\mu}}{\pi\hbar}\int_0^\infty dR \frac{D(R)}{\sqrt[4]{(\varepsilon - V_{\Lambda''}(R,\,Y))(\varepsilon + h\nu - V_{\Lambda'}(R,\,Y))}} \times \cos\left[\phi(Y,\,\varepsilon,\,\nu,\,R)\right], \tag{A.2}$$

where

$$\phi(Y,\,\varepsilon,\,\nu,\,R) = \frac{\sqrt{2\mu}}{\hbar}\left[\int_{R_t'}^{R} dR'\sqrt{\varepsilon - V_{\Lambda'}(R',\,Y)} - \int_{R_t''}^{R} dR'\sqrt{\varepsilon - V_{\Lambda''}(R',\,Y)}\right] \tag{A.3}$$

and R_t's are the respective classical turning points. Expanding the phase function $\phi(Y,\,\varepsilon,\,\nu,\,R)$ around the Condon point(s) $R_i(\nu;\Lambda',\Lambda'') \equiv R_i$ in Taylor series up to the quadratic term(s) and using the stationary-phase approximation, one obtains:

$$\langle \Psi_{\varepsilon,Y,\Lambda''}\,|D(R)|\,\Psi_{\varepsilon+h\nu,Y,\Lambda'}\rangle \approx \frac{\sqrt[4]{2\mu}}{\sqrt{2\pi\hbar}}\sum_i \frac{D(R_i)}{\sqrt[4]{\varepsilon - V_{\Lambda''}(R_i,\,Y)}\sqrt{|W'(R_i)|}} \times \cos\left(\phi(Y,\,\varepsilon,\,\nu,\,R_i) - \sigma_i\frac{\pi}{4}\right), \tag{A.4}$$

where $W(R) = V_{\Lambda'}(R) - V_{\Lambda''}(R)$ is the difference potential, $W'(R) = dW(R)/dR$, and $\sigma_i = \mathrm{sgn}\,[W'(R_i)]$.

We now substitute (A.4) into equation (10) for $I(\nu,\,T)$, with the integrations over Y and ε'' restricted to the classically allowed region. For the cross terms with $R_i \neq R_j$

the common CAR is the intersection of the two respective CAR's for R_i and R_j. Neglecting the rapidly oscillating phase terms of the form $\phi(Y,\,\varepsilon,\,\nu,\,R_i)\,+\,\phi(Y,\,\varepsilon,\,\nu,\,R_j)$, the integral $I(\nu,\,T)$ can be approximated as:

$$I\,(\nu,\,T) \approx h\frac{\sqrt{2\mu}}{2\pi\hbar}\sum_{i,\,j}\frac{D\,(R_i)\,D\,(R_j)}{\sqrt{|W'(R_i)|\;|W'(R_j)|}} \times \int\limits_{\varepsilon_{\min}}^{\infty} d\varepsilon \exp\left(-\frac{\varepsilon}{k_BT}\right) \times \int\limits_{0}^{Y_M(\varepsilon)} dY \frac{\cos\left(\Delta\phi(Y,\,\varepsilon,\,\nu,\,R_i,\,R_j)+\frac{\sigma_i-\sigma_j}{2}\frac{\pi}{2}\right)}{\sqrt[4]{(\varepsilon-V_{\Lambda''}(R_i,\,Y))\;(\varepsilon-V_{\Lambda''}(R_j,\,Y))}}, \tag{A.5}$$

where $\Delta\phi(Y,\varepsilon,\nu,R_i,R_j)=\phi(Y,\varepsilon,\nu,R_i)-\phi(Y,\varepsilon,\nu,R_j)$.

In order to reduce the double integral in (A.5) to a single one *analytically*, one has to choose a single characteristic point for each of the cross terms with $R_i \neq R_j$, whichever lends itself as the most convenient one, and here we choose $R_{ij}=\sqrt{R_iR_j}$. Assuming further that throughout the entire interval $[R_i,\,R_j]$ one has $\varepsilon - V_{\Lambda''}(R,\,Y) \approx \varepsilon - V_{\Lambda''}(R_{ij},\,Y)$ and $h\nu - W(R) \ll \varepsilon - V_{\Lambda''}(R_{ij},Y)$, the phase difference $\Delta\varphi$ can be simplified to:

$$\Delta\phi\,(Y,\,\varepsilon,\nu,R_i,\,R_j)=\frac{\sqrt{2\mu}}{2\hbar\sqrt{\varepsilon - V_{\Lambda''}(R_{ij},\,Y)}} \times \int\limits_{R_j}^{R_i} dR\,[W(R)-h\nu]\,. \tag{A.6}$$

With this approximation, changing the variables of integrations ε and Y to $\varepsilon_{kin}(R_{ij};0) = \varepsilon - V_{\Lambda''}(R_{ij})$ and $\varepsilon_{kin}(R_{ij};Y) = \varepsilon_{kin}(R_{ij};0) - \hbar^2Y/(2\mu R_{ij}^2)$, respectively, and after integrating by parts over $\varepsilon_{kin}(R_{ij};0)$, one obtains:

$$I(\nu,\,T) \approx h\frac{2\mu k_BT}{\hbar^2}\frac{\sqrt{2\mu}}{2\pi\hbar}\sum_{i,\,j}\frac{R_iD(R_i)R_jD(R_j)}{\sqrt{|W'(R_i)|\;|W'(R_j)|}} \times \int\limits_{\varepsilon_{\min}}^{\infty} d\varepsilon \frac{\exp\left(-\frac{\varepsilon}{k_BT}\right)}{\sqrt{\varepsilon - V_{\Lambda''}(R_{ij})}} \times \cos\left(\frac{\sqrt{2\mu}}{2\hbar\sqrt{\varepsilon - V_{\Lambda''}(R_{ij})}}\int\limits_{R_j}^{R_i} dR\,[W(R)-h\nu]+\frac{\sigma_i-\sigma_j}{2}\frac{\pi}{2}\right). \tag{A.7}$$

In the simplest case of a single Condon point R_ν equation (A.7) reduces to:

$$I(\nu,\,T) \approx \left(h\frac{2\mu k_BT}{\hbar^2}\right)\frac{\sqrt{2\mu}}{2\pi\hbar} \times \sqrt{\pi k_BT}\frac{\exp(-V_{\Lambda''}(R_\nu)/k_BT)}{|W'(R_\nu)|}R_\nu^2D(R_\nu)^2, \tag{A.8}$$

which gives one a hint to consider the integral

$$h\frac{2\mu k_BT}{\hbar^2}\int\limits_{\varepsilon_{\min}}^{\infty} d\varepsilon \exp\left(-\frac{\varepsilon}{k_BT}\right) \times \left|\langle\Phi_{\varepsilon,0,\,\Lambda''}\,|RD(R)|\,\Phi_{\varepsilon+h\nu,0,\Lambda'}\rangle\right|^2. \tag{A.9}$$

If one now calculates (A.9) along the same lines as outlined above for $I(\nu,T)$, assuming an arbitrary number of Condon points, one ends up with the same result, i.e., the right-hand side of equation (A.7). This shows that $I(\nu,T)$ and the integral (A.9) have the same semiclassical "limit", for any number of Condon points at that. That is, in the semiclassical region *at least*, one has:

$$I\,(\nu,\,T) \approx h\frac{2\mu k_BT}{\hbar^2}\int\limits_{\varepsilon_{\min}}^{\infty} d\varepsilon \exp\left(-\frac{\varepsilon}{k_BT}\right) \times \left|\langle\Phi_{\varepsilon,0,\,\Lambda''}\,|RD(R)|\,\Phi_{\varepsilon+h\nu,\,0,\,\Lambda'}\rangle\right|^2. \tag{A.10}$$

Note that, although one was prompted to arrive at equation (A.10) by the special case of a single Condon point, it actually proves to cover the general case of an arbitrary number of them.

References

1. H.-K. Chung, K. Kirby, J.F. Babb, Phys. Rev. A **60**, 2002 (1999)
2. H.-K. Chung, K. Kirby, J.F. Babb, Phys. Rev. A **63**, 032516 (2001)
3. L.K. Lam, A. Gallagher, M.M. Hessel, J. Chem. Phys. **66**, 3550 (1977)
4. R.J. Le Roy, R.G. Macdonald, G. Burns, J. Chem. Phys. **65**, 1485 (1976)
5. F. Talbi, M. Bouledroua, K. Alioua, Eur. Phys. J. D **50**, 141 (2008)
6. P.S. Erdman, C.W. Larson, M. Fajardo, K.M. Sando, W.C. Stwalley, J. Quant. Spectrosc. Radiat. Trans. **88**, 447 (2004)
7. R. Beuc, M. Movre, V. Horvatic, C. Vadla, O. Dulieu, M. Aymar, Phys. Rev. A **75**, 032512 (2007)
8. D.T. Colbert, W.H. Miller, J. Chem. Phys. **96**, 1982 (1992)
9. K. Willner, O. Dulieu, F. Masnou-Seeuws, J. Chem. Phys. **120**, 548 (2004)
10. R. Beuc, B. Horvatić, M. Movre, J. Phys. B **43**, 215210 (2010)
11. C. Vadla, R. Beuc, V. Horvatic, M. Movre, A. Quentmeier, K. Niemax, Eur. Phys. J. D **37**, 37 (2006)
12. L. Yan, W. Meyer, unpublished results
13. C. Amiot, J. Mol. Spectrosc. **147**, 370 (1991)
14. C. Amiot, J. Vergès, C.E. Fellows, J. Chem. Phys. **103**, 3350 (1995)
15. M.R. Manaa, A.J. Ross, F. Martin, P. Crozet, A.M. Lyyra, L. Li, C. Amiot, T. Bergeman, J. Chem. Phys. **117**, 11208 (2002)
16. J. Heinze, U. Schühle, F. Engelke, C.D. Caldwell, J. Chem. Phys. **87**, 45 (1987)